Polymer Chemistry

Tuning PNIPAm Self-Assembly and Thermoresponse: Roles of Hydrophobic End-Groups and Hydrophilic Comonomer

Journal:	*Polymer Chemistry*
Manuscript ID	PY-ART-02-2019-000180.R1
Article Type:	Paper
Date Submitted by the Author:	18-Apr-2019
Complete List of Authors:	Ohnsorg, Monica; University of Minnesota, Chemistry Ting, Jeffrey; University of Minnesota, Chemical Engineering Jones, Seamus; University of Minnesota, Chemical Engineering Jung, Seyoung; University of Minnesota, Chemical Engineering Bates, Frank; University of Minnesota, Chemical Engineering Reineke, Theresa; University of Minnesota, Chemistry

SCHOLARONE™
Manuscripts

Tuning PNIPAm Self-Assembly and Thermoresponse: Roles of Hydrophobic End-Groups and Hydrophilic Comonomer

Monica L. Ohnsorg,[†] Jeffery M. Ting,[‡,⊥] Seamus D. Jones,[‡,⊥] Seyoung Jung,[‡] Frank S. Bates, [,‡]*

and Theresa M. Reineke[,†]*

[†]Department of Chemistry, [‡]Departments of Chemical Engineering and Materials Science,

University of Minnesota, Minneapolis, MN 55455

ABSTRACT

Modifications to the aqueous solution self-assembly and thermoresponsive properties of poly(N-isopropylacrylamide) (PNIPAm) can be achieved by hydrophobic end-group functionalization and incorporation of hydrophilic *N,N*-dimethylacrylamide (DMA) repeat units. Although these variations have been studied separately in the past, the simultaneous effects of both modifications have not been investigated systematically. Herein, we report the synthesis of six NIPAM and DMA based statistical, ABA triblock, and ABABA pentablock copolymers using reversible addition-fragmentation chain transfer (RAFT) polymerization, each containing one or two dodecyl hydrocarbon end-groups. Assembly into nanoscale particles and thermoresponsive properties in phosphate buffered saline were studied using light scattering and diffusion ordered NMR spectroscopy. Cloud points (T_{cp}) remained between 30-45 °C, notwithstanding hydrophobic modification. Copolymers with two alkyl tails assembled into flower-like micelles below the T_{cp}. The monofunctional statistical copolymer formed a core-shell assembly and the monofunctional ABA and ABABA polymers were molecularly dissolved. Above the T_{cp}, reversible precipitation was observed in all systems except for the monofunctional ABABA pentablock, which unexpectedly formed uniform large (> 100 nm diameter) aggregates interpreted as mesoglobules. These results demonstrate surprising and delicately balanced tradeoffs between short non-polar end groups and tailored hydrophobicity in the nanoscale self-assembly of PNIPAm based copolymers in water near the lower critical solution temperature.

INTRODUCTION

Among biomaterials, poly(N-isopropylacrylamide) (PNIPAm) represents one of the most extensively investigated stimuli-responsive soft materials to date, as a consequence of its lower critical solution temperature (LCST) in water (~32 °C) enabling control over molecular conformation in physiological conditions.[1–3] When heated above the LCST, PNIPAm undergoes a coil-to-globule transition; the intermolecular polymer-water hydrogen bonding network becomes disrupted by prevailing intramolecular interactions causing chain collapse and aggregation.[4,5] This thermal responsivity has been exploited in PNIPAm containing platforms to sequester/release therapeutic cargo,[6,7] template nanopatterns of protein hybrids,[8] and form hydrogels for tissue regeneration.[9] Almost all of these applications utilize PNIPAm in a block polymer architecture to arrange hierarchical structures at multiple length scales.[10] The phase behavior of block polymers in solution is governed by similar parameters as in the melt (e.g., molecular weight, architecture, topology, solubility parameters); however, the added roles of polymer concentration, solvent quality, pH, and temperature (in the case of thermoresponsive polymers) impacts the size and shape of compartmentalized micelle assemblies, or dictate whether aggregates form at all.[11–14] Since precise control over size and shape is critical for the functionality of biological delivery vehicles, it is essential to develop design rules which can be used to predict nanostructure results as a function of all relevant parameters.[15,16]

In particular, PNIPAm-containing block copolymers can conceivably sequester and release cargo as a "smart nanocarrier" in aqueous media.[7] There are two simple routes to modulate this encapsulation/release behavior: (1) modification of chain termini with hydrophobic moieties to induce self-assembly, and (2) incorporation of hydrophilic comonomers to control chain hydration and thermoresponsivity. Although the impacts of such modifications have been studied separately, the subtle interplay between the utility of self-assembly-inducing hydrophobic end-groups and thermoresponsive modulation using hydrophilic comonomers has not been systematically investigated. In this study, we investigate the balance between hydrophobic and hydrophilic

modification using statistical and multiblock copolymer architectures composed of NIPAm and

N,N-dimethylacrylamide (DMA) with one or two hydrophobic alkyl end-groups.

Since 1997, post-synthetic hydrophobic modifications to PNIPAm chain termini with alkyl

chains have been used to form stable, thermoresponsive structures that can encapsulate

hydrophobic molecules at room temperature.[17] Similar hydrophobically modified PNIPAm (HM-

PNIPAm) systems have been synthesized using reversible addition-fragmentation chain transfer

(RAFT) polymerization to install alkyl ethyl to octadecyl hydrocarbon end-groups as part of the

trithiocarbonate chain transfer agent (CTA).[18] In such systems, successful encapsulation and

solubilization of hydrophobic molecules using HM-PNIPAm has been attributed to the formation

of a stable core-shell micelle structure with a hydrated PNIPAm corona below the LCST.[17,19,20]

HM-PNIPAm with two octadecyl alkyl end-groups, telechelic PNIPAm (*tel*-PNIPAm), has been

observed to form flower-like micelles in aqueous media.[18,21] Meanwhile, PNIPAm

hydrophobically modified through the statistical incorporation of a hydrophobic comonomer forms

loose globular assemblies below the LCST.[22] Collectively, such hydrophobic modifications

promote a *decrease* in the LCST due to end-group or comonomer driven self-assembly seeding

polymer-polymer interactions and thereby increasing the tendency for PNIPAm to structure at

elevated temperatures in water. In other words, the incorporation of hydrophobicity decreases

polymer miscibility in water and reduces the entropy of mixing through micelle or globular

formation promoting phase separation. Lang *et al.* has attributed the drastic reduction in the LSCT

of HM-PNIPAm micelles to de Gennes' n-clustering theory,[23,24] suggesting that a group of three

or more monomers can be attractive in a good solvent – where pair-wise monomer interactions are

otherwise repulsive, driven by a concentration-dependent Flory-Huggins parameter. This leads to

increased polymer-polymer interactions as a consequence of the increased polymer density near

the hydrophobic core.[25]

In addition to this chain localization effect, Lang and coworkers also suggest that the

relative hydrophilicity of the main polymer chain relative to the terminal group affects

thermoresponsive behavior. Block polymers consisting of thermosensitive acrylamides and hydrophilic neutral blocks can assemble by tuning the LCST.[26] Unlike selective solvent driven self-assembly observed in PNIPAm-*b*-polystyrene diblock copolymers[27] and ABCBA multiblock systems (hydrophobic blocks of poly(propylene oxide) and poly(*tert*-butyl acrylate)[28]), the hydrophilic neutral block remains soluble at temperatures above the LSCT, facilitating micelle assembly as a function of temperature upon PNIPAm core collapse. A common hydrophilic modifier with PNIPAm is the comonomer DMA.[9,29–31] We have previously explored compositional effects of NIPAm/DMA RAFT copolymers as solubility enhancing agents for oral drug delivery.[32–34] In these works, the statistical copolymers with a CTA containing a dodecyl alkyl chain end ($-C_{12}H_{25}$) *increased* the cloud point temperature to 37 °C in PBS buffer and up to 55 °C in deionized water.[32] Therefore, DMA incorporation increased the main chain polymer hydrophilicity enough to out-compete any hydrophobic n-clustering effects.

To the extent of our knowledge, this delicate balance between hydrophobic and hydrophilic interactions driving self-assembly and thermoresponsiveness has not been systematically studied. In this work, copolymers of NIPAm and DMA are used to investigate the interplay between hydrophobic end-group driven self-assembly and main chain hydrophilic modification. A better understanding of how end-group driven micellar structures can be constructed in solution without sacrificing thermoresponsivity at physiologically relevant temperatures is of high interest to biological drug carrier applications. We used either a monofunctional (one $-C_{12}H_{25}$ end group) or symmetric bifunctional (two $-C_{12}H_{25}$ end groups) RAFT CTA to prepare statistical, ABA triblock, and ABABA pentablock copolymers at equivalent molecular weights and effective NIPAm/DMA compositions (Figure 1A) to probe the combined effects of hydrophobic end-group associations and main chain hydration. At room temperature, these parameters directly impacted micellization. The effect of the interplay between hydrophobic and hydrophilic modifications on the cloud point was compared (Figure 1B). We demonstrate that a balance between hydrophilic and hydrophobic

modification affords formation of HM-PNIPAm core-shell and flower-like micelles, and even mesoglobules, in aqueous settings.
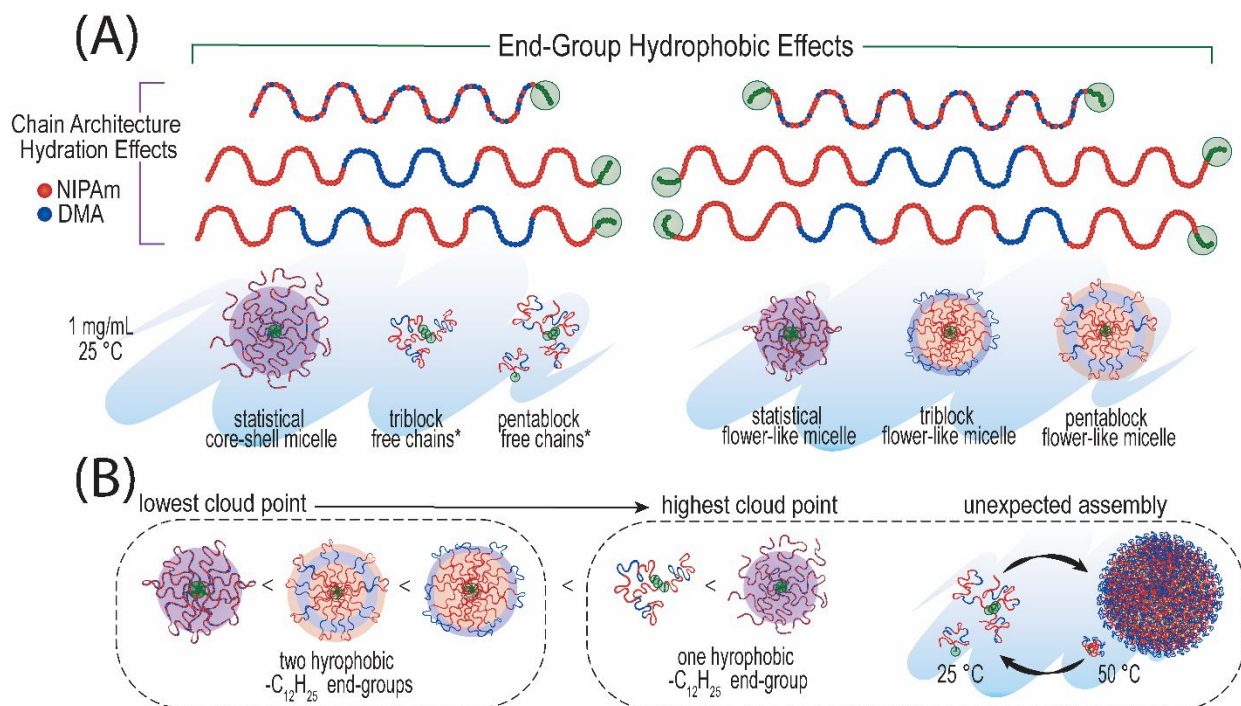
Figure 1. (A) Statistical, ABA triblock, and ABABA pentablock copolymers comprised of equivalent N-isopropylacrylamide (NIPAm, red) and *N,N*-dimethylacrylamide (DMA, blue) compositions synthesized with either one or two hydrophobic $–C_{12}H_{25}$ end-groups (green). Cartoon representations of the aqueous solution structures at 1 mg/mL at 25 °C are shown. *The majority population in solution is free chains; however, there is a small aggregated population (less than 10% by mass) observed by light scattering at 1 mg/mL (See Figure S27). (B) Hydrophobically and hydrophilically modified copolymer systems arranged from lowest to highest cloud point temperature. The pentablock copolymer with a single hydrophobic end-group exhibited unexpected reversible hierarchical assembly at elevated temperatures.

RESULTS & DISCUSSION

Multiblock Synthesis and Characterization

Six copolymers were synthesized via RAFT polymerization using monofunctional and bifunctional CTAs to install either one or two dodecyl hydrocarbon end-groups, respectively. The targeted degree of polymerization (DP) for each block extension was adjusted to maintain total

molecular weights of 15-17 kg/mol and chemical compositions of 70 mol% NIPAm to stay consistent with the poly(NIPAm-*co*-DMA) copolymer prepared in previous work.[32] For nomenclature of these materials, triblocks and pentablocks are respectively represented as $N_aD_bN_c$ and $N_aD_bN_cD_dN_e$, where the italicized subscripts denote the DP of each corresponding block of NIPAm (N) and DMA (D) calculated by NMR. Block copolymer samples were targeted to be $N_{48}D_{41}N_{48}$ and $N_{32}D_{20}N_{32}D_{20}N_{32}$, so that the theoretical molecular weights and effective chemical compositions were similar between multiblock systems, but the architectural arrangement of blocks differed.

Scheme 1 shows representative synthesis steps for the three copolymer architectures and using both CTAs (see Supporting Information Section 1.1 for Materials, Synthetic Procedures, and Characterization Details). The statistical copolymers poly(N-*co*-D)$_{107}$-C12 (Scheme 1A) and C12-poly(N-*co*-D)$_{129}$-C12 (Scheme 1B) were synthesized in 1,4-dioxane at 70 °C with AIBN and either 2-(dodecylthiocarbonothioylthio) propionic acid (DoPAT[35]) or the bifunctional RAFT CTA 3,5-bis(2-dodecylthiocarbonothioylthio-1-oxopropoxy) benzoic acid (BDOBA[36]), and NIPAm /DMA monomers. The triblock and pentablock copolymer systems were synthesized by sequential chain extensions of either NIPAm or DMA under otherwise-identical reaction conditions (Scheme 1). The use of DoPAT imparts a single alkyl hydrophobic –$C_{12}H_{25}$ tail (Scheme 1A,1C, and 1E), whereas the BDOBA CTA translates into the inclusion of –$C_{12}H_{25}$ tails on both living chain ends (Scheme 1B, 1D, and 1F). Polymerizations were conducted for t = 18 h with 2,2'-azobis(2-methylpropionitrile) (AIBN), and the initial CTA to initiator ratio ($[CTA]_0 / [I]_0$) was maintained at 10:1 for all reactions. The theoretical number fraction of living chains (L)[37], or the number of retained thiocarbonylthio moieties needed for chain extension, was calculated to be ~97% (See Supporting Information Section 1.1 for calculation details).

Scheme 1. General RAFT reaction scheme used for each polymerization and sequential block extension. Chemical structures of the statistical, triblock, and pentablock copolymers. (A) poly(N-co-D)$_{107}$-C12, (B) C12-poly(N-co-D)$_{129}$-C12, (C) N$_{52}$D$_{50}$N$_{41}$-C12, (D) C12-N$_{69}$D$_{60}$N$_{69}$-C12, (E) N$_{35}$D$_{40}$N$_{42}$D$_{23}$N$_{22}$-C12, (F) C12-N$_{46}$D$_{29}$N$_{46}$D$_{29}$N$_{46}$-C12.
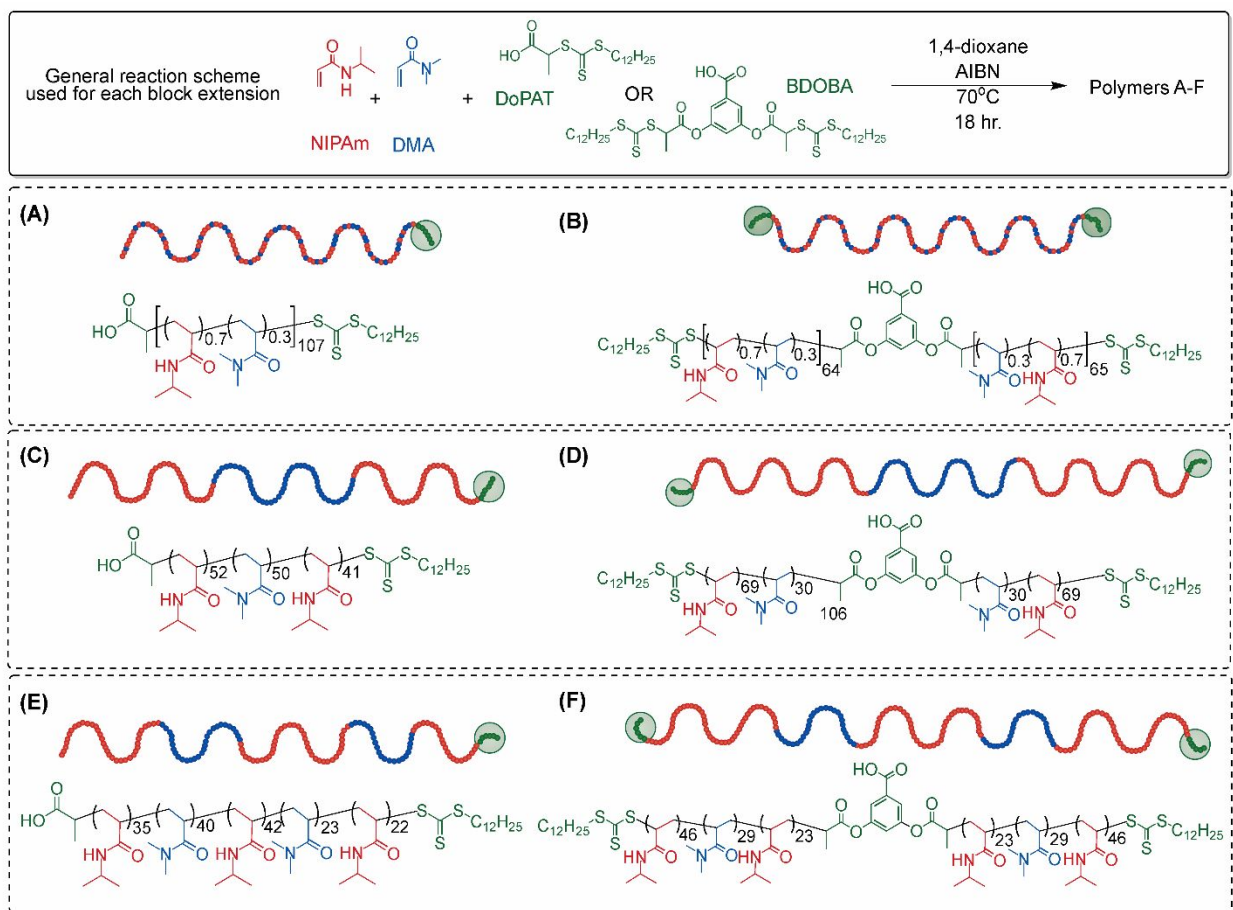
Table 1 summarizes the characterization of the polymer absolute number-average molecular weight (M_n), dispersity ($Đ$), and molar composition of each polymer at each block extension using size-exclusion chromatography with multi-angle light scattering (SEC-MALS) (See Supporting Information Section 1.2 for details and dn/dc calculations) and ^{1}H NMR spectroscopy in CDCl$_3$. Across all six systems, the molecular weight distributions remained relatively narrow ($Đ$ < 1.2), and the changing M_n and chemical composition confirmed RAFT chain-extension. The M_n of the monofunctional and difunctional CTA derived statistical copolymers (poly(N-co-D)$_{107}$-C12 and C12-poly(N-co-D)$_{129}$-C12) were 11.6 and 14.0 kg/mol with

$Đ$ of 1.03 and 1.06, respectively (Fig. S1). Figures S2 through S5 show the progression of ^{1}H NMR spectra of the purified polymer used to determine molar polymer composition of all multiblock copolymers, and Table S1 summaries the calculated dn/dc for each block extension. Figures S6 and S7 plot the evolution of these parameters upon each block extension. The final polymer molecular weight (11-13 kg/mol, with $Đ$ < 1.2) and chemical compositions (65-70 mol % NIPAm) for the triblocks ($N_{52}D_{50}N_{41}$-C12 and C12-$N_{69}D_{60}N_{69}$-C12) and pentablocks ($N_{35}D_{40}N_{42}D_{23}N_{22}$-C12 and C12-$N_{46}D_{29}N_{46}D_{29}N_{46}$-C12) were approximately equivalent.

Table 1. Molecular characterization summary of prepared multiblock polymers.

	System [a]	Block Extension No.	M_n [b] (g/mol)	Đ [c]	Polymer Comp [d] (mol %, N/D)
A	poly(N-co-D)$_{107}$-C12	N/A	11,600 [e]	1.03	63/37
B	C12-poly(N-co-D)$_{129}$-C12	N/A	14,000 [e]	1.06	66/34
		1	6230	1.02	100/0
C	N$_{52}$D$_{50}$N$_{41}$-C12	2	8750	1.13	51/49
		3	12,200	1.12	65/35
D	C12-N$_{69}$D$_{60}$N$_{69}$-C12	1	6720	1.02	100/0
		2	12,800	1.06	70/30
		1	4340	1.05	100/0
		2	5740	1.17	47/53
E	N$_{35}$D$_{40}$N$_{42}$D$_{23}$N$_{22}$-C12	3	10,000	1.06	66/34
		4	11,300	1.08	55/45
		5	11,700	1.15	61/39
		1	6050	1.02	100/0
F	C12-N$_{46}$D$_{29}$N$_{46}$D$_{29}$N$_{46}$-C12	2	7180	1.06	44/56
		3	12,400	1.09	70/30

[a] Nomenclature for triblocks (NDN) and pentablocks (NDNDN) of NIPAm (N) and DMA (D); the subscripted numbers denote the degree of polymerization of each corresponding block, based on ^{1}H NMR spectroscopy/SEC analysis and assuming one RAFT agent per chain. The C12 represents the R-C$_{12}$H$_{25}$ chain end depending on the selected RAFT chain transfer agent. [b] Absolute number-average molecular weight (M_n), determined from SEC using THF as the elutant at 25 °C and the theoretical dn/dc values (see Equation S2). [c] Dispersity (Đ) = M_w/M_n. [d] Molar polymer composition of NIPAm and DMA, determined from ^{1}H NMR spectroscopy of the purified polymer. [e] Determined from SEC using DMF + 0.05 M LiBr as the elutant at 50 °C (due to column pressure issues with the THF SEC-MALS) and reported dn/dc values in the Supporting Information.

An overlay of the SEC traces shows similar elution times of the final multiblocks (Figure 2). For both triblock polymers, SEC-MALS traces revealed distinct monomodal shifts to higher molecular weights upon each block addition (Figure 2A and 2B). However, the molecular weight distribution of the pentablock copolymer, $N_{35}D_{40}N_{42}D_{23}N_{22}$-C12, exhibited a low-molecular weight shoulder at the third block addition (Figure 2C). We observed that the shoulder elution time remained constant through the next two block extensions and thus likely represented terminated chains, which lack an alkyl end-group. By comparison, the synthesis of the symmetric C12-$N_{46}D_{29}N_{46}D_{29}N_{46}$-C12 from BDOBA resulted in clear monomodal shifts in the SEC elution (Figure 2D).
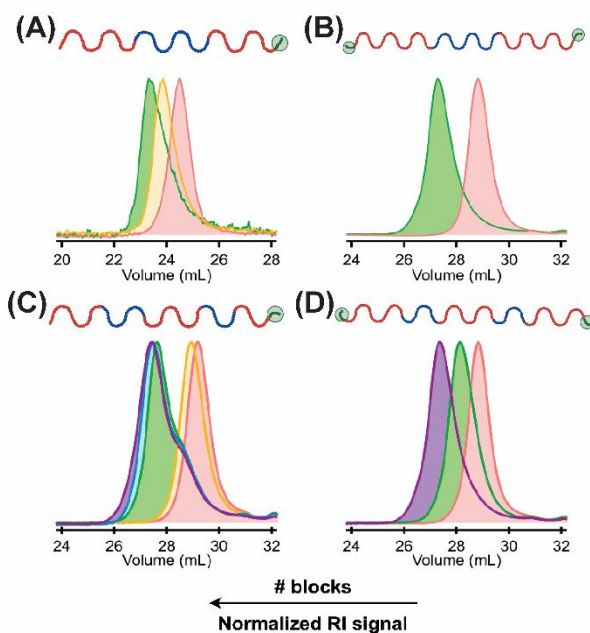
Figure 2. Gallery of SEC RI traces for multiblock systems. The overlays include each block extension for (A) $N_{52}D_{50}N_{41}$-C12, (B) C12-$N_{69}D_{60}N_{69}$-C12, (C) $N_{35}D_{40}N_{42}D_{23}N_{22}$-C12, and (D) C12-$N_{46}D_{29}N_{46}D_{29}N_{46}$-C12. Blocks one, two, three, four, and five of each system correspond to the colors red, orange, green, blue, and purple, respectively. Due to symmetric block extension for (B) and (D), the green trace represents the increase in molecular weight with the addition blocks two and three, and purple represents the extension of blocks four and five.

Physical Effects of Hydrophobic End-Group and Hydrophilic Comonomer Incorporation

Cloud Point Modulation. Cloud point measurements were conducted using an in-house HeNe laser transmission instrument from which the transmitted intensity was recorded as a function of temperature upon heating (Figure 3, closed circles) and cooling (Figure 3, open circles). The observed cloud point temperature (T_{CP}) was defined by a sharp loss in sample transmittance with equally abrupt recovery of sample transmittance upon cooling. Further experimental details, photos, and videos are recorded in the Supporting Information Sections 1.3 and 3.1. Each cloud point sample was dissolved at a concentration of 1 mg/mL in aqueous buffer (PBS, pH = 6.5). Previous work with HM-PNIPAm has elucidated a decrease in T_{CP} due to increased hydrophobicity of the polymer chains.[22,38–40] However, in systems which formed stable core-shell micelles, driven by the hydrophobicity of dodecyl- or octadecyl-hydrocarbon end-groups, minimal change in T_{CP} was observed compared to unmodified PNIPAm as the micellar structure protected the hydrophobic core with a PNIPAm corona.[17,39,41,42] Therefore, with core-shell micelle formation, the T_{CP} of the dodecyl hydrocarbon end-group and hydrophilically modified systems should not decrease below that of linear unmodified PNIPAm. In fact, for the poly(N-co-D)$_{107}$-C12 sample, the T_{CP} was observed to increase to 46 °C with only 30 mol% statistical incorporation of the hydrophilic comonomer, DMA. The triblock copolymer with one hydrophobic end-group, N$_{52}$D$_{50}$N$_{41}$-C12, behaved similarly with a rapid loss in transmittance at 45 °C and recovery of transmittance upon cooling. However, N$_{52}$D$_{50}$N$_{41}$-C12 exhibited greater hysteresis upon cooling than the statistical copolymer system, poly(N-co-D)$_{107}$-C12. These two cases show that, in the case of single end-group hydrophobic modification, the incorporation of a hydrophilic comonomer increases the T_{CP} above that of the PNIPAm homopolymer (T_{CP} = ~32 °C).

The abrupt transmittance recovery upon cooling observed for poly(N-co-D)$_{107}$-C12 was delayed upon cooling for the N$_{52}$D$_{50}$N$_{41}$-C12 system. Selective hydrophobic collapse of the PNIPAm blocks upon heating for triblock copolymer is hypothesized to disrupt the hydrophobic, alkyl end-group core to induce formation of larger aggregates upon heating as PNIPAm oligomers of n > 16 have been modeled to be able to undergo a coil-to-globule transition.[43] This would result in the observed hysteresis upon cooling as triblock copolymer chains rearrange to re-form a stable hydrophobic hydrocarbon core solubilized by the hydrophilic triblock copolymer corona.
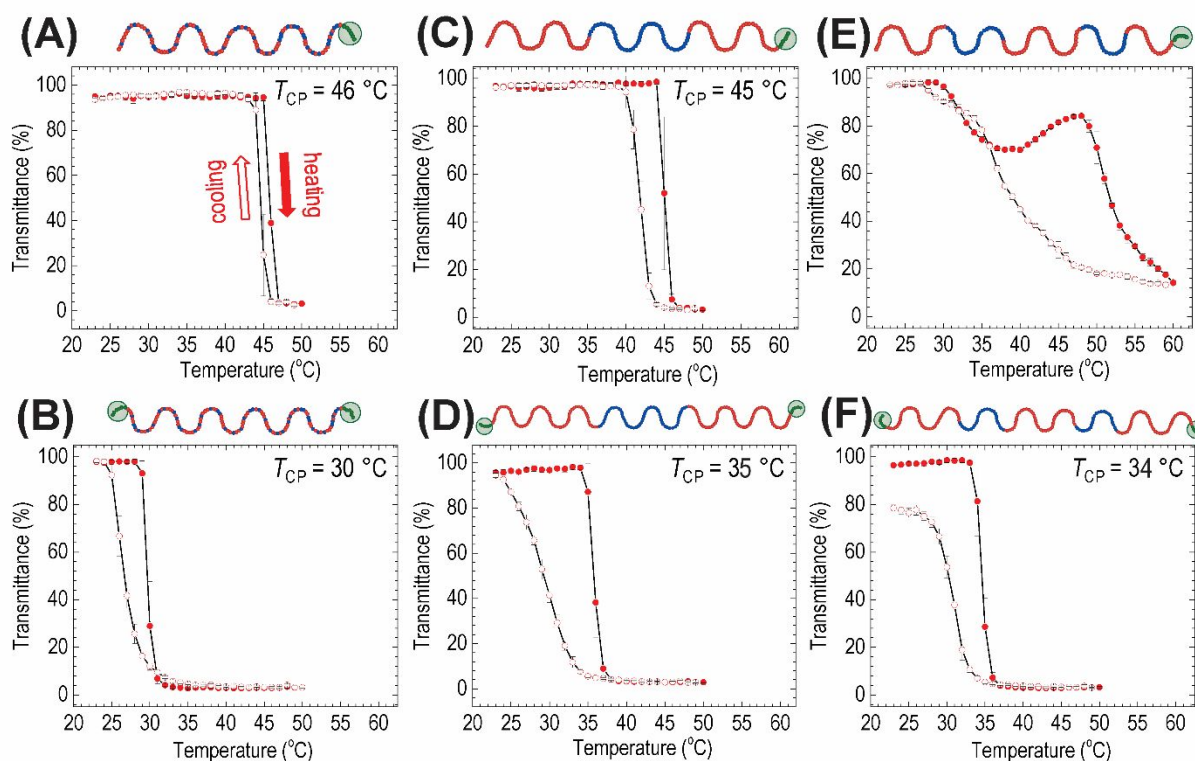
Figure 3. Cloud point curves upon heating (filled, red circles and arrow) and cooling (open, red circles and arrow) of investigated multiblocks (A) poly(N-*co*-D)$_{107}$-C12, (B) C12-poly(N-*co*-D)$_{129}$-C12, (C) N$_{52}$D$_{50}$N$_{41}$-C12, (D) C12-N$_{69}$D$_{60}$N$_{69}$-C12, (E) N$_{35}$D$_{40}$N$_{42}$D$_{23}$N$_{22}$-C12, and (F) C12-N$_{46}$D$_{29}$N$_{46}$D$_{29}$N$_{46}$-C12. Samples, at a concentration of 1 mg/mL, were heated at a rate of 0.25 °C/min and cooled under ambient conditions. The cloud point was defined as the temperature when the solution transmittance decreased to less than 80% of the value for the fully dissolved solution. Data points and vertical error bars denote the average and standard deviation, respectively, of over N = 30 measurements at each temperature.

In all cases, the incorporation of a second hydrophobic end-group reduced the T_{CP}, compared the monofunctional CTA derived analogs. The T_{CP} for C12-poly(N-*co*-D)$_{129}$-C12, C12-N$_{69}$D$_{60}$N$_{69}$-C12, and C12-N$_{46}$D$_{29}$N$_{46}$D$_{29}$N$_{46}$-C12 were reduced to 30, 34, and 35 °C, respectively (Figure 3B, D, and F). This decreases in T_{CP} despite hydrophilic comonomer incorporation as has been observed for *tel*-PNIPAm systems with two octadecyl hydrocarbon chain ends which associated to form flower-like micelles.[18,21,25] Theory from Semenov *et al.* has explained the tendency of flower-like micelles to form loose associations with each other driven by the high probability of bridging.[44] A similar postulation for the T_{CP} reduction in *tel*-NIPAm/DMA statistical and block copolymer systems states that the increased chain density surrounding the core of a flower-like micelle system increases the probability for the isopropyl groups on the NIPAm units to form small hydrophobic domains below the T_{CP}.[23] Such "clusters" formed by the triads and tetrads of repeating NIPAm units in the statistical copolymer analogue[24] and the PNIPAm end blocks of both the triblock and pentablock copolymer systems would increase the initial hydrophobicity through dehydration of the flower-like micellar core even before heating.

Hysteresis in transmittance recovery was observed for these samples, most evident in sample C12-N$_{46}$D$_{29}$N$_{46}$D$_{29}$N$_{46}$-C12 which does not fully regain 100% transmittance upon cooling (Figure 3F). Therefore, inspired by the work of Semenov *et al.* and Koga *et al.*,[21,44] it is hypothesized that mesoglobules (colloidally stable structures composed of >1000 polymer chains) form at high temperatures due to the preliminary collapse of the NIPAm units near the core in all three systems to form multilayered flower-like micelle structures with NIPAm "clusters" near the hydrophobic core and swollen DMA and NIPAm units around the corona. The T_{CP} trends are visualized in Figure 1B. Notably, end-group identity has the greatest observable effect on the thermoresponsivity of the statistical copolymers, which exhibit both the highest and lowest T_{CP},

differing only by the presence of one end-group. It is hypothesized that for poly(N-co-D)$_{107}$-C12, a stable core-shell micellar system exists in solution resulting in minimal disruption to the hydrophobic core upon heating. In contrast, the low barrier to bridging and aggregation in the flower-like micelle forming C12-poly(N-*co*-D)$_{129}$-C12 system increases the tendency to form micelle-rich and polymer-lean domains in solution decreasing the T_{CP}. The following section describes diffusion-measurement techniques used to further interrogate this hypothesis. Characterizing the solution structures at room temperature lead us to a potential mechanism for thermoresponsiveness caused by hydrophobic end-group driven self-assembly and the architecture of hydrophilic comonomer incorporation.

The pentablock copolymer derived from the monofunctional CTA did not exhibit a single T_{CP} like the other samples. This anomalous cloud point behavior prompted further temperature dependent light scattering studies in order to elucidate the thermoresponsive mechanism. A report of double thermosensitivity by Savoji *et al.* in a NIPAm-containing statistical block copolymer demonstrates the possibility of a single polymer which exhibits two T_{CP}'s due to differing NIPAm incorporations in each block.[26] This explanation is not sufficient for N$_{35}$D$_{40}$N$_{42}$D$_{23}$N$_{22}$-C12, as the multi-cloud point behavior emerged only upon the 5th block extension. This suggests a solution structure contingent on the pentablock copolymer architecture is driving the double T_{CP} behavior.

Dynamic light scattering measurements were collected as a function of temperature using identical solution conditions (1 mg/mL) to the T_{CP} measurement studies. The distribution of measured hydrodynamic radii present in solution is plotted as a function of temperature and overlaid with the transmittance data upon heating in Figure 4B. The distribution of hydrodynamic radii as a function of temperature from 25 to 50 °C is shown in Figure 4C, determined via a

regularized positive exponential sum (REPES) Laplace inversion route analysis[45] of the generated autocorrelation function at a scattering angle of 90°.

At room temperature, the solution exists as two populations in solution, free chains with R_h equal to 4.5 nm and a population of aggregated chains (R_h = 67.0 nm). The polymer self-assembles into a single population of aggregates at 31 °C (R_h =99 nm), swells to nearly twice this size at 36 °C, then collapses to a narrowly disperse population (R_h = 65 nm) at 42 °C before stabilizing to 58 nm-sized particles at 50 °C. We interpret the unusual drop in transmittance as corresponding to the presence of the R_h = 99 nm population at 36 °C, with increased transmittance when the self-assembled structure decreases in size and the population distribution sharpens. Upon cleavage of the dodecyl chain end using aminolysis and Michael addition of methylacrylate (See Supporting Information Section 2.3), the same cloud point behavior was observed (Figure S12), and the same solution structure was formed at 50 °C as shown in the overlaid REPES plot in Figure S24. This indicates that thermoresponsiveness is due to the hydrophilically-modified block copolymer structure alone, and not a result of hydrophobic modification.
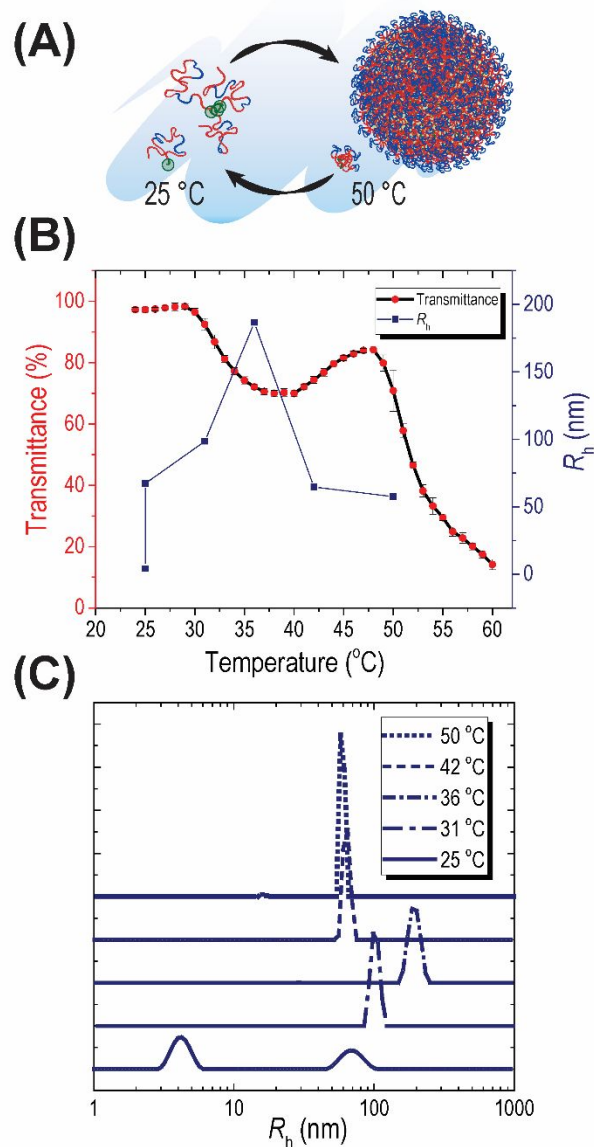
Figure 4. Thermoresponsive behavior of $N_{35}D_{40}N_{42}D_{23}N_{22}$-C12. (A) Illustration of hypothesized solution structures at room temperature and 50 °C. (B) Comparison of particle size, R_h (right y-axis, blue) and transmittance (left y-axis, red; error bars denote the standard deviation of N = 30 measurements at each temperature) upon heating the samples from 25 °C to 60 °C. (C) Dynamic light scattering data processed by REPES analysis showing apparent hydrodynamic radius distributions as a function of temperature. Data has been z-shifted for clarity.

Static light scattering approximations were used to glean more information about the solution structure of the well-defined species present at 50 °C. Figure 4A illustrates the hypothesized thermoresponsive solution structures of $N_{35}D_{40}N_{42}D_{23}N_{22}$-C12 where PDMA blocks

(blue) stabilize the outside of a large aggregate driven by the hydrophobic collapse of PNIPAm blocks (red). The weight-average molecular weight (M_w) of the aggregate species present in solution at 50 °C was measured using partial Zimm approximations (Figure S14). This revealed that the structure contained ~ 1000 polymer chains per aggregate. Using the R_g calculated from static light scattering (SLS) approximations, M_w of the aggregate, and R_h determine by DLS, the aggregate was calculated to have a density of 0.04 g/mL and shape factor (R_g / R_h) of 0.54 (Supporting Information Section 4.1). This suggests the structure is highly solvated. Small shape factors, when the R_g is greater than the R_h – specifically equal to 0.6, less than 0.77 expected for a hard sphere – have been associated with vesicle structures in solution.[46] Therefore, it is hypothesized this structure could either be a swollen collection of aggregates or a vesicle-like structure with an outer shell of approximately 800 chains and the remainder of the pentablock copolymers trapped inside the outer shell.

The characterized system parallels that of the solution structures Koga *et al.* observed from a *tel*-PNIPAm, C18-PNIPAm-C18, using small-angle neutron scattering. Upon heating the *tel*-PNIPAm system to 30 °C, the formation of a mesoglobule consisting of 1000 polymer chains with a radius of ~20 nm was oberseved.[21] Therefore, it is hypothesized the pentablock copolymer forms structures similar to the observed mesoglobules. However, this assembly formation at elevated temperatures for the $N_{35}D_{40}N_{42}D_{23}N_{22}$-C12 system is not a result of end-group driven flower-like micellization, but of the PNIPAm end blocks driving micellization at elevated temperatures. The low concentration (1 mg/mL) of the system ensures no associations between mesoglobules and instead of passing through a flower-like micelle intermediate, similar to the *tel*-PNIPAm system, the linear chains (R_h = 4.5 nm) assemble directly to form large aggregates which stabilize into monodisperse ($\mu_2/\Gamma^2 < 0.1$, see Supporting Information Section 1.3) mesoglobules with R_h equal

to 58 nm above 42 °C. Unfortunately, attempts to characterize these particles by small-angle X-ray scattering and cryogenic imaging were unsuccessful due to the poor contrast of the low-density solvated particles in aqueous buffer at 50 °C (Supporting Information Section 4.2). The formation of such mesoglobule structures is inherently distinct from typical cloud point behavior observed by variable-temperature DLS measurements for the three other multiblock copolymer samples (Figure S23). In each case, as the sample approaches its cloud point, the particle size narrows as the PNIPAm blocks undergo a coil-to-globule transition preferring self-interactions over solvent-interactions; then, the formation of micron sized particles is indicative of a turbid solution as shown in Figure S9 at 50 °C. The solutions exist with polymer poor and polymer rich phases tending towards total phase separation. Therefore, to the authors' knowledge, $N_{35}D_{40}N_{42}D_{23}N_{22}$-C12 at 50 °C is the first demonstration of mesoglobule formation in a *hydrophilically* modified PNIPAm system *without* the pre-formation of flower-like micelles by hydrophobic end-groups.

Solution Structure Formation

To better understand how the seed structures of each copolymer system influenced the corresponding thermoresponsive properties, we aimed to characterize the assembly structure as a function of polymer concentration with multi-angle DLS at room temperature. The hydrodynamic radius of each system at a concentration of 1 mg/mL measured by both DOSY-NMR and DLS is given in Table 2. The statistical copolymers each formed narrowly disperse solution structures at 1 mg/mL in solution. The poly(N-co-D)$_{107}$-C12 system was observed to form a stable core-shell micelle (R_h = 9.3 nm). The bifunctional statistical analogue existed as a single population (R_h = 7.3 nm) at 1 mg/mL understood to be a flower-like micellar structure.[47] Both the monofunctional triblock and pentablock copolymers existed as free chains with a detectable population of large aggregates (R_h = 6.0, 34.0 and 4.5, 67.0, respectively). As shown in Figure S26, the aggregate

population makes up less than 10% of the R_h distribution by mass for the triblock and less than 1% by mass for the pentablock. Alternatively, the bifunctional triblock and pentablock copolymers formed single populations of flower-like micelles in solution, like the statistical copolymer analogue, with hydrodynamic radii equal to 9.8 and 10.4 nm, respectively. The size of the solution populations of the multiblock copolymers was corroborated with diffusion ordered spectroscopy NMR (DOSY-NMR) to measure the diffusion coefficient and the Stokes-Einstein relationship. (See Supporting Information Section 4.3 for fits and calculations). DOSY-NMR analysis of these systems only detected the presence of faster diffusing, free chains which would be the dominant species in solution (Table 2 and Figures S18 and S19). The preceding data gives insight into the seed structures present in solution at temperatures below the T_{CP}.

Table 2. Room temperature characterization aqueous solution characterization.

	System	$R_{h, DOSY}{}^{a}$ (nm)	$R_{h, DLS}$ (nm)	μ_2/Γ^{2} ^{d}
A	poly(N-co-D)$_{107}$-C12	N/A	9.3 ^{c}	0.20
B	C12-poly(N-*co*-D)$_{129}$-C12	N/A	7.3 ^{c}	0.13
C	N$_{52}$D$_{50}$N$_{41}$-C12	6.0	6.0, 34.0 ^{b}	-
D	C12-N$_{69}$D$_{60}$N$_{69}$-C12	10.4	10.4 ^{c}	0.09
E	N$_{35}$D$_{40}$N$_{42}$D$_{23}$N$_{22}$-C12	5.2	4.5, 67.0 ^{b}	-
F	C12-N$_{46}$D$_{29}$N$_{46}$D$_{29}$N$_{46}$-C12	9.8	10.4 ^{c}	0.12

[a] Average hydrodynamic radius, measured by DOSY-NMR. [b] Average hydrodynamic radius, measured by DLS and analyzed with REPES Laplace inversion route analysis. [c] Average hydrodynamic radius, measured by DLS and determined by a cumulant expression fitting the correlation function. [d] Polydispersity measured via DLS at the 90° scattering angle, defined as μ_2/Γ^2 (See Supporting Information Section 1.3).

To probe the relative importance of end-group effects and block structural effects on self-assembly, the trithiocarbonate end-groups of C12-$N_{69}D_{60}N_{69}$-C12 were cleaved using sequential aminolysis and Michael addition of methyl acrylate. After cleavage of the two hydrophobic end-groups, the cloud point was retested. It was observed to increase 2 °C and the hysteresis upon cooling was diminished (Figure S13). When analyzed in solution at 1 mg/mL at 25 °C, the sample no longer existed as a single population, but formed two populations (R_h equal to 3 nm and 50 nm) which persisted up to a concentration of 10 mg/mL (Figure S25). The same multimodal distribution of aggregates was observed for the mono-hydrophobically modified systems, $N_{52}D_{50}N_{41}$-C12 and $N_{35}D_{40}N_{42}D_{23}N_{22}$-C12, at 1 mg/mL in Figure 5C and 5E.

The size distributions of each system in aqueous buffer at concentrations from 1-25 mg/mL are shown in Figure 5. Poly(N-co-D)$_{107}$-C12 formed a core-shell micelle with $R_h = 9.3$ nm, stable in solution at all investigated concentrations (Figure 5A). This confirms the hypothesis that a stable core-shell micellar system exists in solution resulting in minimal disruption to the hydrophobic core upon heating. When two hydrophobic end-groups were added to the statistical copolymer, in the case of C12-poly(N-co-D)$_{129}$-C12, the polymer forms an aggregate with $R_h = 7.3$ nm at low concentrations, assumed to be a flower-like micelle based on previous hydrophobic-modification work.[18,21,44,48] However, consistent with theory proposed by Semenov et $al.$,[44] with increasing concentration, the flower-like micelles begin to bridge forming polymer-rich and polymer-poor domains in solution illustrated by population broadening around 10 mg/mL the emergence of a larger aggregate population at 20 mg/mL ($R_h = 13$ nm and 45 nm). This same trend is observed for both bifunctional CTA derived triblock and pentablock copolymers C12-$N_{69}D_{60}N_{69}$-C12 and C12-$N_{46}D_{29}N_{46}D_{29}N_{46}$-C12, which exhibited a single solution population with $R_h = 9.8$ and 10.4

nm, respectively, and low colloidal polydispersity at low concentrations for both samples (See

Table 2).

Partial Zimm approximations determined that there were 19 and 18 polymer chains per

aggregate in polymers $C12\text{-}N_{69}D_{60}N_{69}\text{-}C12$ and $C12\text{-}N_{46}D_{29}N_{46}D_{29}N_{46}\text{-}C12$, respectively

(Supporting Information Section 4.1). The number of chains per aggregate mirrors that of the

literature C18-PNIPAm-C18 system at $T < T_{CP}$ where about 12 polymer chains were measured to

assemble into a flower-like micelle.[21] At high concentrations, the formation of bridged, larger

aggregates drives gelation of the samples at elevated temperatures.[21,48] This was observed for 25

mg/mL solutions of $C12\text{-}N_{69}D_{60}N_{69}\text{-}C12$ and $C12\text{-}N_{46}D_{29}N_{46}D_{29}N_{46}\text{-}C12$ at 50 °C in PBS buffer

(See photos in Figure S11). Interestingly, despite the hydrophilic comonomer incorporation, the

polymer systems with two hydrophobic end-groups follow the solution behavior of the PNIPAm

homopolymer models. The solution self-assembly and aggregation is independent of copolymer

microstructure or DMA incorporation, and the T_{CP} remains unchanged compared to linear

PNIPAm homopolymers for the statistical copolymer but increases 5 °C for the multiblock

copolymer systems.
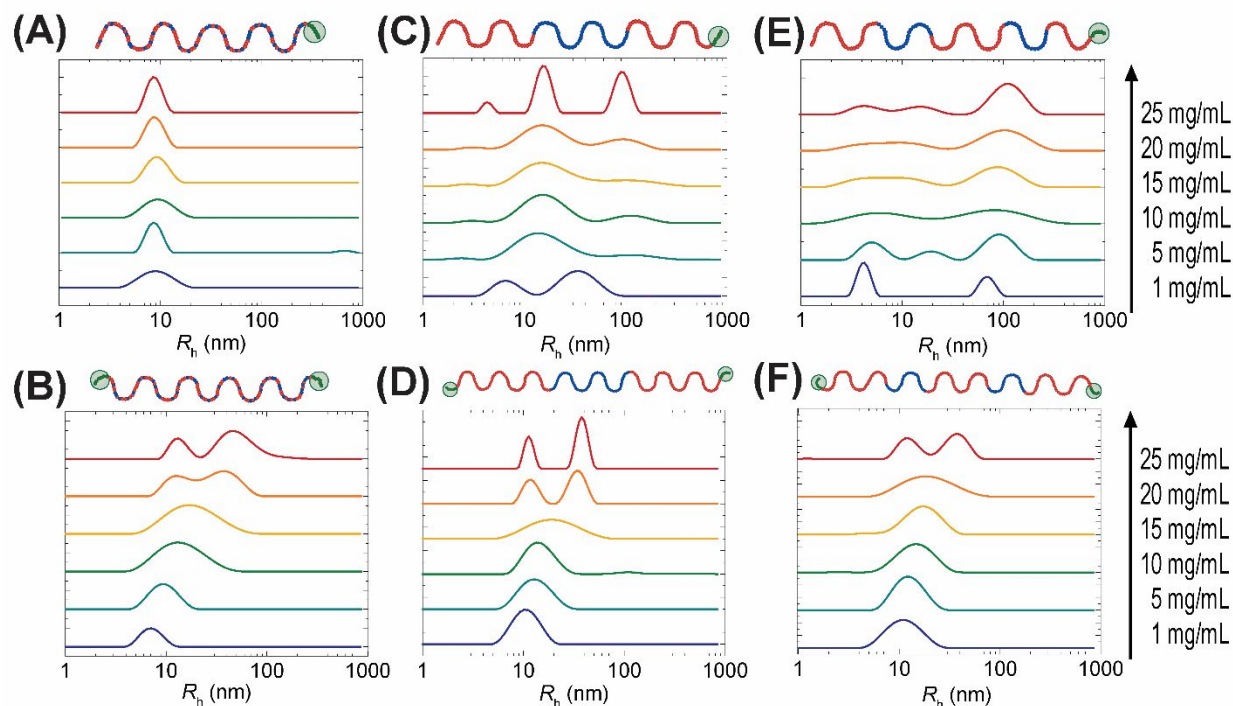
Figure 5. Apparent hydrodynamic radius distributions of multiblock systems in PBS solution at 25°C for (A) poly(N-*co*-D)$_{107}$-C12, (B) C12-poly(N-*co*-D)$_{129}$-C12, (C) N$_{52}$D$_{50}$N$_{41}$-C12, (D) C12-N$_{69}$D$_{60}$N$_{69}$-C12, (E) N$_{35}$D$_{40}$N$_{42}$D$_{23}$N$_{22}$-C12, and (F) C12-N$_{46}$D$_{29}$N$_{46}$D$_{29}$N$_{46}$-C12. The normalized curves at increasing polymer concentration from 1 to 25 mg/mL were vertically shifted for clarity. The 90° scattering angle was selected for DLS REPES analyses.

The monofunctional multiblock copolymers, N$_{52}$D$_{50}$N$_{41}$-C12 and N$_{35}$D$_{40}$N$_{42}$D$_{23}$N$_{22}$-C12, severely aggregate into three populations at concentrations of 1-25 mg/mL in Figures 5C and 5E. The aggregation is theorized to be a result of intramolecular clustering driven by n-clustering associations between NIPAm units driven together by weak hydrophobic associations of the dodecyl chain ends in aqueous buffer. In addition, each PNIPAm block in these multiblock systems can be thought of as a low molecular weight homopolymer. Reduction in molecular weight has been demonstrated to lower the LCST of PNIPAm homopolymers with hydrophobic end groups.[40] Therefore, each PNIPAm block may exist close to its T_{CP} at 25 °C leading to increased hydrophobicity of the block and increased self and intramolecular interactions in aqueous environments driving aggregation. In the case of the pentablock, N$_{35}$D$_{40}$N$_{42}$D$_{23}$N$_{22}$-C12, the aggregation of the PNIPAm blocks at 1 mg/mL primes the linear polymer-to-mesoglobule transition at elevated temperatures. Elucidating room temperature assembly assesses the 1) impact

23

of hydrophobic modification on polymer chains in solution and 2) role of monomer arrangement on solution stability.

CONCLUSIONS

In this study, a library of statistical, triblock, and pentablock copolymers was synthesized to study the interplay of hydrophilic and hydrophobic PNIPAm modification. Rigorous solution-phase characterization was employed to probe the thermoresponsive behavior of these architecturally distinct systems. Light scattering and diffusion-ordered NMR studies were used to determine the self-assembled structures in aqueous conditions. Altogether, this allowed the identification of dominating effects in solution at room and elevated temperatures to better inform the design of responsive drug carrier systems in biological settings.

The following design rules can be gleaned from the discussion above: 1) Low incorporations of hydrophilic comonomer, regardless of architecture, can increase the cloud point of hydrophobically modified PNIPAm systems to above or close to biologically relevant temperatures. 2) The mesoglobule formation theories and trends associated with *tel*-PNIPAm systems hold true for hydrophilically modified systems with two hydrophobic end-groups regardless of copolymer microstructure at elevated temperatures. In this study, 30 wt% incorporation of a hydrophilic comonomer was observed to increase the measured T_{CP} by ~10 °C. 3) Block copolymer architectures with one hydrophobic end-group aggregate at low temperatures and concentrations due to weak hydrophobic end-group associations promoting n-clustering driven aggregation of PNIPAm blocks. 4) In the case of $N_{35}D_{40}N_{42}D_{23}N_{22}$-C12, the unusual thermoresponsiveness observed demonstrates that tailored block architecture, beyond diblock and triblock architectures and regardless of end-groups, can drive the formation of hierarchical, self-assembled structures at high temperatures in solution. By better understanding the balance between hydrophobic and hydrophilic modifications to polymers in aqueous conditions, future studies will

focus on how to harness n-clustering effects to drive the formation of more tailored, complex thermoresponsive solution structures as a function of end-group and comonomer incorporation.

CONFLICTS OF INTEREST

There are no conflicts to declare.

AUTHOR INFORMATION

Corresponding Author

*E-mail: F. S. B.: bates001@umn.edu; T. M. R.: treineke@umn.edu

Present Addresses

⊥ J.M.T.: Institute for Molecular Engineering, University of Chicago, Chicago, Illinois 60637, United States; S.D.J.: Departments of Chemical Engineering and Materials, University of California, Santa Barbara, California 93117, United States.

REFERENCES

1   H. G. Schild, *Prog. Polym. Sci.*, 1992, **17**, 163–249.

2   Y. Xia, X. Yin, N. A. D. Burke and H. D. H. Stöver, *Macromolecules*, 2005, **38**, 5937–
        5943.

3   X. Wang, X. Qiu and C. Wu, *Macromolecules*, 1998, **31**, 2972–2976.

4   S. Fujishige, K. Kubota and I. Ando, *J. Phys. Chem.*, 1989, **93**, 3311–3313.

5   A. Halperin, M. Kröger and F. M. Winnik, *Angew. Chemie - Int. Ed.*, 2015, **54**, 15342–
        15367.

6   D. Yang, G. Yang, S. Gai, F. He, R. Lv, Y. Dai and P. Yang, *ACS Biomater. Sci. Eng.*, 2016,
        2, 2058–2071.

7   C. Y. Kuo, Y. C. Wang, C. F. Lee and W. Y. Chiu, *J. Polym. Sci. Part A Polym. Chem.*,
        2014, **52**, 561–571.

8   B. Kim, C. N. Lam and B. D. Olsen, *Macromolecules*, 2012, **45**, 4572–4580.

9   S. E. Kirkland, R. M. Hensarling, S. D. McConaughy, Y. Guo, W. L. Jarrett and C. L.
        McCormick, *Biomacromolecules*, 2008, **9**, 481–486.

10   C. M. Bates and F. S. Bates, *Macromolecules*, 2017, **50**, 3–22.

11   J. Lu, F. S. Bates and T. P. Lodge, *Macromolecules*, 2015, **48**, 2667–2676.

12   H. Qiu, Z. M. Hudson, M. A. Winnik and I. Manners, *Science*, 2015, **347**, 1329–1332.

13   G. Riess, *Prog. Polym. Sci.*, 2003, **28**, 1107–1170.

14   R. K. O'Reilly, C. J. Hawker and K. L. Wooley, *Chem. Soc. Rev.*, 2006, **35**, 1068–1083.

15   H. Acar, J. M. Ting, S. Srivastava, J. L. LaBelle and M. V. Tirrell, *Chem. Soc. Rev.*, 2017,

46, 6553–6569.

16   A. O. Moughton, M. A. Hillmyer and T. P. Lodge, *Macromolecules*, 2012, **45**, 2–19.

17   J. E. Chung, M. Yokoyama, K. Suzuki, T. Aoyagi, Y. Sakurai and T. Okano, *Colloids Surfaces B Biointerfaces*, 1997, **9**, 37–48.

18   P. Kujawa, F. Segui, S. Shaban, C. Diab, Y. Okada, F. Tanaka and F. M. Winnik, *Macromolecules*, 2006, **39**, 341–348.

19   L. M. Johnson, Z. Li, A. J. LaBelle, F. S. Bates, T. P. Lodge and M. A. Hillmyer, *Macromolecules*, 2017, **50**, 1102–1112.

20   Z. Li, L. M. Johnson, R. G. Ricarte, L. J. Yao, M. A. Hillmyer, F. S. Bates and T. P. Lodge, *Langmuir*, 2017, **33**, 2837–2848.

21   T. Koga, F. Tanaka, R. Motokawa, S. Koizumi and F. M. Winnik, *Macromolecular*, 2008, **291**–**292**, 177–185.

22   Z. Cao, W. Liu, P. Gao, K. Yao, H. Li and G. Wang, *Polymer*, 2005, **46**, 5268–5277.

23   P. G. de Gennes, *C. R. Adad. Sci., Ser. II Mec., Phys., Chim., Sci. Terre Univers*, 1991, **313**, 1117–1122.

24   K. Turner, P. W. Zhu and D. H. Napper, *Colloid Polym. Sci.*, 1996, **274**, 622–627.

25   X. Lang, A. D. Patrick, B. Hammouda and M. J. A. Hore, *Polymer*, 2018, **145**, 137–147.

26   M. T. Savoji, S. Strandman and X. X. Zhu, *Macromolecules*, 2012, **45**, 2001–2006.

27   S. Kessel, N. P. Truong, Z. Jia and M. J. Monteiro, *J. Polym. Sci. Part A Polym. Chem.*, 2012, **50**, 4879–4887.

28   C. Lv, Z. Zhang, J. Gao, J. Xue, J. Li, J. Nie, J. Xu and B. Du, *Macromolecules*, 2018, **51**, 10136–10149.

29 A. J. Convertine, B. S. Lokitz, Y. Vasileva, L. J. Myrick, C. W. Scales, A. B. Lowe and C. L. McCormick, *Macromolecules*, 2006, **39**, 1724–1730.

30 C. A. Figg, A. Simula, K. A. Gebre, B. S. Tucker, D. M. Haddleton and B. S. Sumerlin, *Chem. Sci.*, 2015, **6**, 1230–1236.

31 C. A. Figg, R. N. Carmean, K. C. Bentz, S. Mukherjee, D. A. Savin and B. S. Sumerlin, *Macromolecules*, 2017, **50**, 935–943.

32 J. M. Ting, S. Tale, A. A. Purchel, S. D. Jones, L. Widanapathirana, Z. P. Tolstyka, L. Guo, S. J. Guillaudeu, F. S. Bates and T. M. Reineke, *ACS Cent. Sci.*, 2016, **2**, 748–755.

33 Z. Li, T. I. Lenk, L. J. Yao, F. S. Bates and T. P. Lodge, *Macromolecules*, 2018, **51**, 540–551.

34 Z. Li, N. J. Van Zee, F. S. Bates and T. P. Lodge, *ACS Nano*, 2019, acsnano.8b06393.

35 G. Moad and J. Chiefari, RAFT: Choosing the Right Agent to Achieve Controlled Polmerization, www.sigmaaldrich.com, (accessed 20 April 2018).

36 M. Nasiri and T. M. Reineke, *Polym. Chem.*, 2016, **7**, 5233–5240.

37 G. Gody, T. Maschmeyer, P. B. Zetterlund and S. Perrier, *Macromolecules*, 2014, **47**, 639–649.

38 P. Kujawa and F. M. Winnik, *Macromolecules*, 2001, **34**, 4130–4135.

39 P. A. Fitzgerald, S. Gupta, K. Wood, S. Perrier and G. G. Warr, *Langmuir*, 2014, **30**, 7986–7992.

40 X. Qiu, T. Koga, F. Tanaka and F. M. Winnik, *Sci. China Chem.*, 2013, **56**, 56–64.

41 F. M. Winnik, A. Adronov and H. Kitano, *Can. J. Chem*, 1995, **73**, 2030–2040.

42 F. M. Winnik, A. R. Davidson, G. K. Hamer and H. Kitano, *Macromolecules*, 1992, **25**,

1876–1880.

43   T. E. De Oliveira, C. M. Marques and P. A. Netz, *Phys. Chem. Chem. Phys.*, 2018, **20**, 10100–10107.

44   A. N. Semenov, J. F. Joanny and A. R. Khokhlov, *Macromolecules*, 1995, **28**, 1066–1075.

45   J. Jakeš, *Collect. Czechoslov. Chem. Commun.*, 1995, **60**, 1781–1797.

46   M. Kesimer and R. Gupta, *Methods*, 2015, **87**, 59–63.

47   R. Nojima, T. Sato, X. Qiu and F. M. Winnik, *Macromolecules*, 2008, **41**, 292–294.

48   M. A. Winnik and A. Yekta, *Curr. Opin. Colloid Interface Sci.*, 1997, **2**, 424–436.
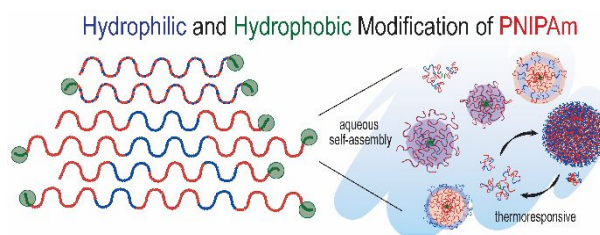
Summary of Novelty:

Systematic study of hydrophobic and hydrophilic modifications to poly(N-isopropylacrylamide) elucidates design rules for control over cloud point and aqueous self-assembly.